Title
STEADY STATE CREEP OF A SUPERPLASTIC LEAD-TIN EUTECTIC ALLOY AT LOW STRESS

Authors
Grivas, D.I.
Morris, J.W.

Publication Date
1973-12-01

Submitted to Metallurgical Transactions

LBL-2532
Preprint c.2

STEADY STATE CREEP OF A SUPERPLASTIC LEAD-TIN EUTECTIC ALLOY AT LOW STRESS

D. I. Grivas and J. W. Morris, Jr.

December 1973

Prepared for the U. S. Atomic Energy Commission
under Contract W-7405-ENG-48

DISCLAIMER

STEADY STATE CREEP OF A SUPERPLASTIC LEAD-TIN EUTECTIC ALLOY AT LOW STRESS

by

D. I. Grivas and J. W. Morris, Jr.
Department of Materials Science and Engineering,
University of California and Center for the Design of Alloys,
Inorganic Materials Research Division, Lawrence Berkeley Laboratory,
Berkeley, California 94720

ABSTRACT

The steady-state creep rates of the superplastic lead-tin eutectic alloy were measured over a stress range of 2.2 psi to 468 psi. Creep tests were performed on specimens with grain sizes ranging from 2.8 μm to 6.7 μm and temperatures from 98°C to 168°C. Over these experimental variables two different creep behaviors were observed. At higher stresses the conditions for superplastic creep were satisfied. The lower stress region was found to obey the equation

$$\dot{\gamma}^* = 3.2 \times 10^{12} \tau^{*3} d^{*-2.1} e^{18,900/RT}.$$

The form of this equation is incompatable with both the Coble and Nabarro-Herring creep mechanisms, which have been suggested as dominant mechanisms at low stress.

INTRODUCTION

The mechanism for the steady state creep deformation of superplastic alloys is not fully understood. Bird et al.[1] have proposed that the semi-emprical equation

$$\dot{\gamma}^* = A\tau^{*n} d^{*-m} e^{-\Delta H^*/RT} \qquad (1)$$

with the proper choice of the constants m, n, A and ΔH^*, can represent the creep data for superplastic materials very satisfactorily. In this equation $\dot{\gamma}^*$, τ^*, d^* are as defined in the appendix, the dimensionless shear strain rate, shear stress and grain size, respectively; ΔH^* is the activation energy for creep and n, m, and A represent constants. Various investigators have suggested[1,2,3] that over a wide range of stresses in a plot of strain rate vs stress there exists regions of constant n values, in each of which a different mechanism dominates the steady state creep rate.

In a recent publication[4] we found that equation 1 represented the high temperature creep data for the superplastic Pb-Sn eutectic alloy very satisfactorily. We also found that the steady state creep data broke into two distinct regions satisfying different variants of Eq. (1) with different values for the exponent n, m and ΔH^*. In the high stress creep region the values for $n = 7.1$, $m = 0$, $A = 1.3 \times 10^{15}$ and $\Delta H^* = 19.4$ kcal/mole seemed to satisfy the conditions suggested for the climb of dislocations to be the controlling mechanism[1]. For the lower creep region the stress exponent (n) was found to be equal to 2, fulfilling the requirements for superplastic behavior[5]. The activation energy was of the order of grain boundary diffusion and the constants took the values n=2, m=1.8 and A=900.

Various researchers[1,2,3,6,7] have suggested that at still lower stresses another region will intrude, in which the creep rate will be controlled by a diffusional mechanism. These diffusional mechanism can be either of the type suggested by Coble,[6] which involves atom movement through grain boundaries and hence requires an activation energy equal to that for grain boundary diffusion; or of the type introduced by Nabarro[7] which involves lattice diffusion and requires an activation energy equal to that for self diffusion. Both models suggest a value for the stress exponent (n) equal to one, with a grain size dependence d^{*-3} for Coble creep and d^{*-2} for Nabarro creep.

The creep behavior at low stresses is controversial. Bird et al.[1] analyzed existing data on superplastic Al-Zn eutectoid and Pb-Sn eutectic. They found evidence for Coble creep in Al-Zn, but were unable to establish its existence in the Pb-Sn eutectic due to the unavailability of low-stress data. They suggested that for all superplastic materials, Coble creep is the dominant mechanism at low stresses. While both Vaidya et al[8] and Misro et al[9] have reported the presence of Coble creep in eutectoid Al-Zn, others[10] have disputed altogether the idea of diffusional creep on experimental grounds. The limited existing data on the Pb-Sn eutectic[11,12] reveals a stress exponent in this region much higher than 1, more on the order of 3. Such a value for n would exclude any of the above mentioned diffusional processes.

The present research was undertaken to obtain more data in the low stress creep region and to investigate the transition from the superplastic to the low stress creep region for the Pb-Sn eutectic alloy. Following the results presented in[4], Eq. (1) will be used to represent the present data.

EXPERIMENTAL PROCEDURE

Pb-62Sn eutectic alloy was prepared from 99.9% pure tin and 99.9% pure lead. The alloy was cast in a graphite crucible to 2.5" diameter, and reduced to 7/8" diameter rods by a sequence of reductions at -44°C. From these rods double shear specimens[13] were machined. Annealing the specimens at 170°C for 1.25, 7, 12, and 17 hours resulted in 2.8 μm, 4.3 μm, 5.8 μm, and 6.7 μm grain size respectively. These grain sizes were determined by the mean intercept method[14] from scanning electron micrographs. The specimens were kept at -40°C at all times prior to testing to prevent extensive grain growth. At room temperature creep tests were performed on a constant load creep machine[15]. A silicon oil bath was used to control the temperature which was maintained constant to $\pm 1^{\circ}$C. One specimen was used to obtain all the data for every temperature in a particular grain size excepting the 6.7 μm where 2 specimens were tested at the same temperature.

RESULTS

Tests were performed over a temperature range of 98°C to 168°C and a stress range from 2.2 psi to 468 psi.

Figure 1 is a plot of the measured strain rate $\dot{\gamma}$ against the applied stress for the 5.7 μm grain size at various temperatures. For each temperature the data naturally break into two distinct regions of different slope. The higher stress creep region has a slope ~ 2; the low stress creep region has a slope ~ 3. Indications of this behavior have already been reported elsewhere[11, 12]. Given $n \sim 2$, the higher stress creep region fulfills the condition for superplastic behavior[5], and will be referred to as the superplastic region. Fig. 2 is a typical plot for the computation of the steady state strain rate. As can be seen from this plot primary creep is present in the low stress tests but was not found in the superplastic region. These regions hence seem associated with different controlling mechanisms. Assuming that Eq. (1) applies to each one of these two regions, by chosing the proper values for m, n, A and ΔH^* we can obtain constitutive equations that describe the creep behavior of this alloy. In the next paragraphs we compute these parameters for each of the two regions.

1. Low Stress Region

Examining Eq. (1), it can be seen that the activation energy for creep deformation in this region at constant stress and grain size may be found from the slope of the plot of $\ln\dot{\gamma}T$ against $1/T$. A plot of this kind for the 5.7 μm specimen is shown in Fig. 3. A slight curvature may be noticed. We found previously[4] a similar curvature in a plot of the same kind for the superplastic regionof Pb-Sn eutectic. We suggested then that ΔH^* might depend on some experimental parameter which is a function of temperature. While in the previous study the $\frac{\partial \dot{\gamma}T}{\partial 1/T}$ was found positive in the present case it is negative. Previous work on Pb-Sn eutectic has not been reported for this region in sufficient detail to compare this observation. A least squares analysis through the experimental points revealed an average activation energy equal to 18.9 ± .5 kcal/mole. This value is equal within experimental error to the value 19.4 ± .4 kcal/mole[4] we obtained for conventional creep at higher stresses. This value is of the order of the activation energy for self diffusion[4].

Once the activation energy has been computed, one can make a composite plot of $\ln\dot{\gamma}^* e^{\Delta H^*/RT}$ against $\ln\tau^*$, compensating for the temperature dependence of the strain rate $\dot{\gamma}^*$ to the applied stress τ^*. Such a plot is shown in Fig. 4 for the 5.7 μm grain size. The points of all temperatures essentially coalesced to give a straight line of slope equal to 3.0 ± .1. Fig. 5 is the same kind of plot for the other three grain sizes studied in this investigation. Three parallel lines can be seen, each giving the behavior for a specific grain size.

Judging from Fig. 5 there seems to be a grain size dependence of the creep rate at constant load. The power of this dependence can be obtained from a plot of $\ln\dot{\gamma}^*$ against $\ln d$ at constant τ^*. This plot is shown in Fig. 6. A value of 2.1 ± .1 is obtained, indicating a grain size dependence $\sim d^{*-2}$. To complete the determination of the constitutive equation we require values for A and n. These can be obtained from a plot of strain rate against stress, compensating for both the temperature and grain size dependence. Such a plot is shown in Fig. 7 where we have plotted $\ln\dot{\gamma}^* d^{*m} e^{\Delta H^*/RT}$ against $\ln\tau^*$. The fit seems good, datum points for all temperatures and grain sizes essentially coalesced to give a straight line. A least squares analysis through these points revealed a value for $n = 3.0 \pm .1$ and for A an average value of 3.2×10^{12}.

A constitutive equation for the low stress creep region may now be written in the form of Eq. (1):

$$\dot{\gamma}^* = 3.2 \times 10^{12} \tau^{*3} d^{*-2.1} e^{18,900/RT}$$

As mentioned in the introduction many investigators believe that the controlling mechanism at lower stresses is a diffusional mechanism. Our finding of 1) an activation energy of 18.9 kcal/mole, 2) a grain size dependence $\sim d^{*-2}$, 3) primary creep, and 4) an n value equal to 3, leads us to suggest that another mechanism must be involved for the creep behavior of this alloy at these stresses and grain sizes.

In Fig. 8 we have plotted $\ln\tau^*$ against $\ln\dot{\gamma}^*$ for the low stress creep region for the two extreme grain sizes. We have also estimated the rate of hypothetical Coble creep, using equations given by Bird et al[1]. With the 2.8 μm grain size specimen we tried to observe Coble creep but were unable to go to stresses low enough due to limitations of the apparatus. Although two points fall below the Coble creep curve, the uncertainty in the precise form of the equation governing Coble creep in this material precludes a conclusion that it does not occur. It is, however, conclusive that some mechanism other than those introduced by Coble and Nabarro controls the creep rate at stresses below those at which superplastic creep is observed.

Weertman[16] has suggested a model for low stress creep deformation involving dislocation movement from subgrain boundaries. This mechanism leads to an n value equal to 3 and an activation energy of the order of that for self diffusion, but involves no grain size dependence. The present results are in good agreement with this model except for the grain size dependence. However, the grain size dependence we observed may not indicate an explicit dependence on grain size, but rather an implicit dependence through some other parameter which varied with the grain size in our tests. Such a hidden parameter may be the dislocation density, subgrain boundary morphology, or other variables of microstructural state dependent on the annealing history of the specimen.

2. Superplastic Region

Data gathered in the superplastic region yielded essentially the same activation energy and stress exponent as reported in reference 4 where a more detailed discussion may be found.

Fig. 9 is a plot of $\ln\dot{\gamma}T$ vs $\frac{1}{T}$ for the computation of the activation energy for the creep deformation in this region. A value of 12.2 ± .3 kcal/mole was obtained. This value compares with the value of 11.5 kcal/mole obtained in ref. 4. A temperature compensating plot for the 5.7 μm grain size of $\ln\dot{\gamma}^* \exp(\Delta H^*/RT)$ against $\ln\tau^*$ is shown in Fig. 2. Data at all four temperatures come together to give a straight line of slope 2.0 ± .1. Fig. 10 is a similar plot for the three other grain sizes. Again three parallel lines can be observed, each one corresponding to a particular grain size.

The specimen of this alloy exhibited rapid grain growth at the test temperatures used. In this investigation the applied loads were increased during testing to obtain strain rates in the superplastic region at higher values of the applied stress. In the previous investigation the initial loads applied were in the superplastic region. Since grain growth occurred during testing, the actual sample grain size for tests in the superplastic region is uncertain. Hence we could not obtain a valid independent measure of the grain size dependence. Assuming m =2 and $\Delta H^* = 11.5$ kcal/mole a least squares analysis through the points given by plotting $\ln\dot{\gamma}^* d^{*m} e^{\Delta H^*/RT}$ against $\ln\tau^*$ revealed a value for $A = 5000$ and for $n = 2.1 \pm .1$. This value for A is much higher than the value 209 reported in Ref. 4, against our expectations that an increase in grain size would decrease the strain rate. This shift of the A value may be attributed to any one of three factors: 1) a difference in purity between the specimen in the two investigations; 2) the difference in testing method, described above; 3) the difference in the preparation procedure to obtain the desired grain sizes. While in this study the specimens were reduced at -44°C from 2.5 inches in diameter to 7/8 inch in diameter, in the work reported in Ref. 4 the specimens were reduced at room temperature from 1 inch to 7/8 inch. This severe reduction at low temperature gave smaller initial grain size. Annealing these specimens to obtain the mentioned grain sizes could result in more equiaxed grains yielding a higher creep rate at constant load. Microscopic observations tend to support the expectation of more equiaxed grains.

In our previous report we suggested that superposition of data from various investigators would be dubious since we found that the results of the various investigators are inconsistent with one another. If, as now appears, the value of A depends on the history of the specimen, this inconsistency can be explained. The previous investigators used different processes to obtain their initial microstructures[11,12,17].

ACKNOWLEDGEMENT

The work reported here was supported by the U. S. Atomic Energy Commission through the Inorganic Materials Research Division of the Lawrence Berkeley Laboratory.

APPENDIX

The quantities appearing in equation (1) are defined as follows:

$\dot{\gamma}^* = \dot{\gamma}kT/D_oGb$ (a dimensionless strain rate).

$\tau^* = \tau/G$ (a dimensionless shear stress).

$d^* = d/b$ (a dimensionless grain size).

The symbols have the following meanings:

$\dot{\gamma}$ = strain rate.

k = Boltzman's constant.

T = absolute temperature.

D_o = a characteristic diffusivity, chosen equal to the pre-exponential D_o in the diffusion equation for pure Sn, $(.08\,\mathrm{cm}^2/\mathrm{sec})^{(15)}$.

G = a characteristic stress, taken equal to the shear modulus of pure Sn, $(2 \times 10^{11}(d/\mathrm{cm}))^{(15)}$.

b = a characteristic length, taken equal to the Burger's vector of pure Sn, $(3.18\ (\mathrm{A}))^{(15)}$.

τ = resolved shear stress.

d = mean grain diameter.

REFERENCES

1. J. E. Bird, A. K. Mukherjee and J. E. Dorn, Qualitative Relations Between Properties and Microstructure, Israel University Press, Haifa, (1969) pp. 255-342.
2. O. D. Sherby and R. M. Burke, Prog. Mat. Sci., 13, (1967), p. 325.
3. R. Lagnerborg, Inter. Met. Reviews, 17, (1972), P. 130.
4. D. J. Grivas, K. L. Murty and J. W. Morris, Jr., LBL Report #2519, Lawrence Berkeley Laboratory, Berkeley, Ca. 94720, (1973) (submitted).
5. G. J. Davies, J. W. Edington, C. P. Cutler and K. A. Padmanabham, Mat. Sci. J., 5, 1091, (1970).
6. R. L. Coble, J. Appl Phys., 34, p. 1679, (1970).
7. F. R. Nabarro, Report of a Conference on the Strength of Solids, The Physical Society, London (1948), p. 75.
8. M. L. Vaidya, K. L. Murty and J. E. Dorn, Acta. Met., 21, 1616 (1973).
9. I. Misro and J. K. Mukherjee, Rate Processes in Plastic Deformation, J. C. M. Li, ed., Plenum Press (in press).
10. R. Lagherborg and R. A. Hermo, Mat. Sci. J., 4, 195, (1969).
11. H. E. Cline and T. H. Alden, Trans. Met. Soc. AIME, 239, 710, (1967).
12. Z. W. Zehr and W. A. Backofen, Trans. ASM, 61, 300, (1968).
13. K. L. Murty, F. A. Mohamed and J. E. Dorn, Acta. Met., 20, p. 1009, (1972).
14. F. Schuckher, in Quantitative Microscopy, ed. by R. T. DeHoff and F. N. Phines, McGraw-Hill (1968), p. 233.
15. F. A. Mohamed, PhD Thesis, Department of Materials Science and Engineering, University of California, Berkeley, (1972), LBL Report #1153, November 1972.

16. J. Weertman, *Trans. ASM* *61*, 681 (1968).

17. D. H. Avery and W. A. Backofen, *Trans*, *ASM*, *58*, 551 (1965).

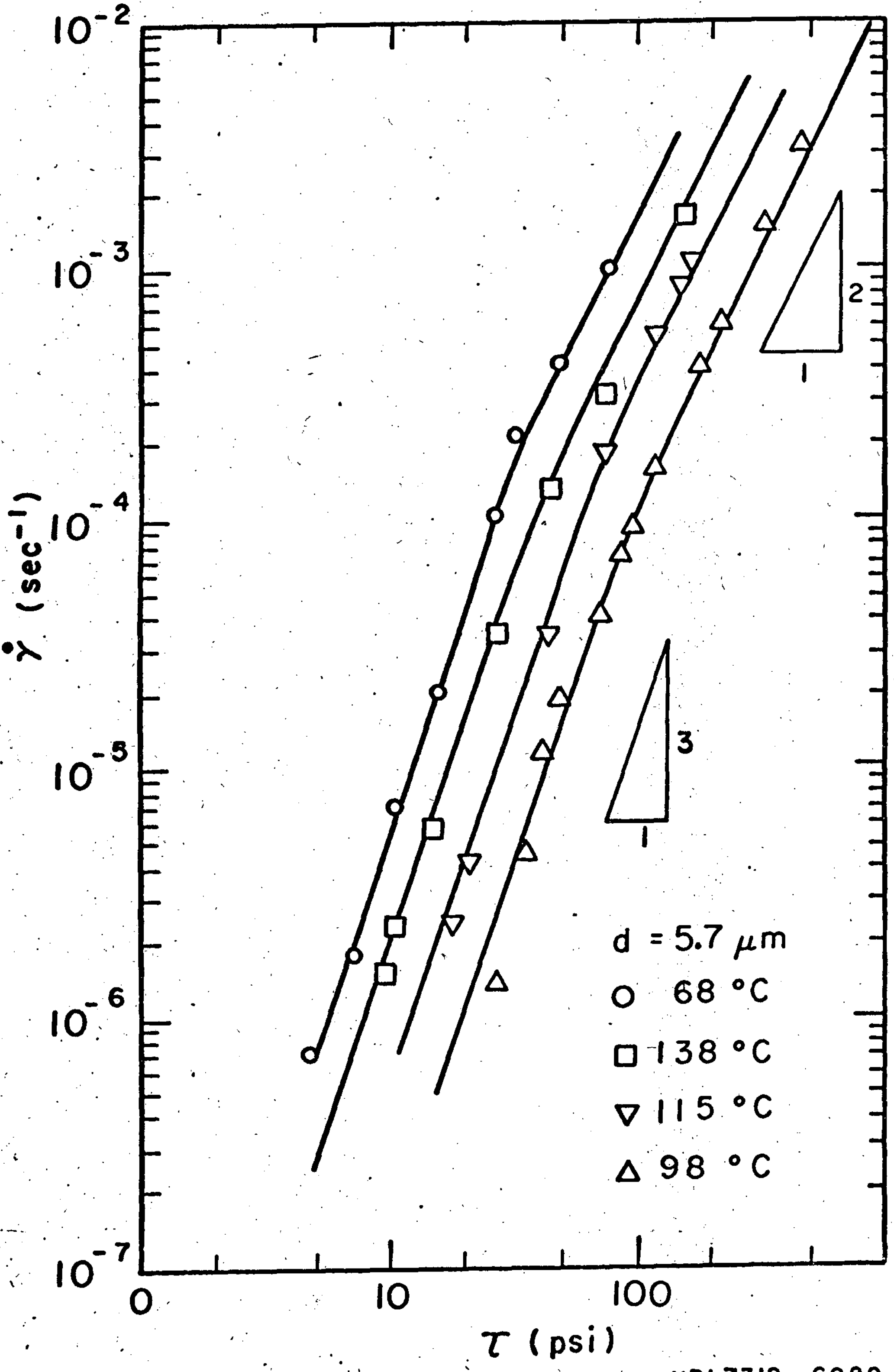

XBL7312-6989

Fig. 1. Stress vs steady-state strain rate for 5.7 μm grain size diameter at various temperatures. Two distinct regions of steady-state creep are revealed.

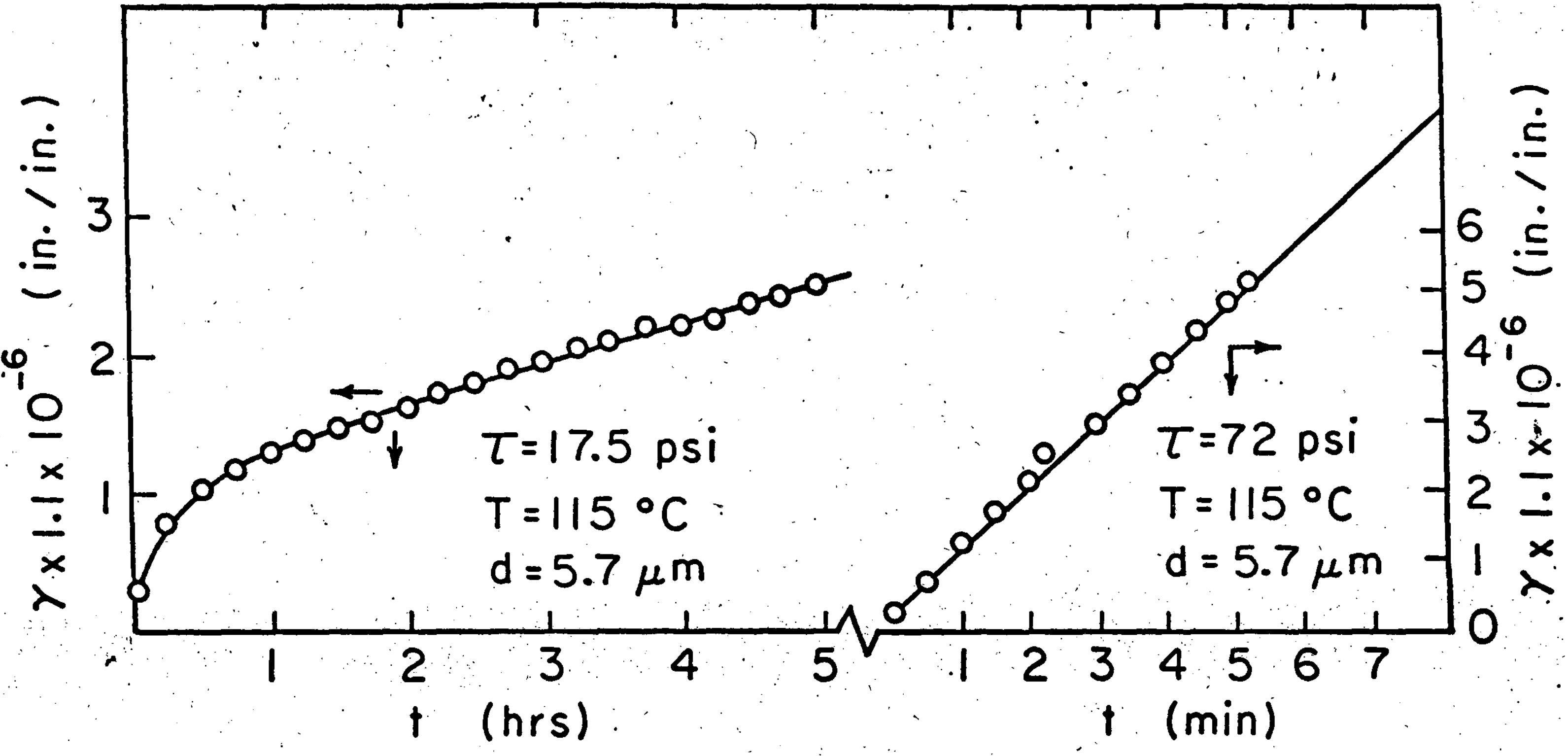

XBL7312-6986

Fig. 2. A typical plot for the determination of the steady-state creep rate. Notice the primary creep for the low stress creep in contrast to the absence of primary creep at higher stresses.

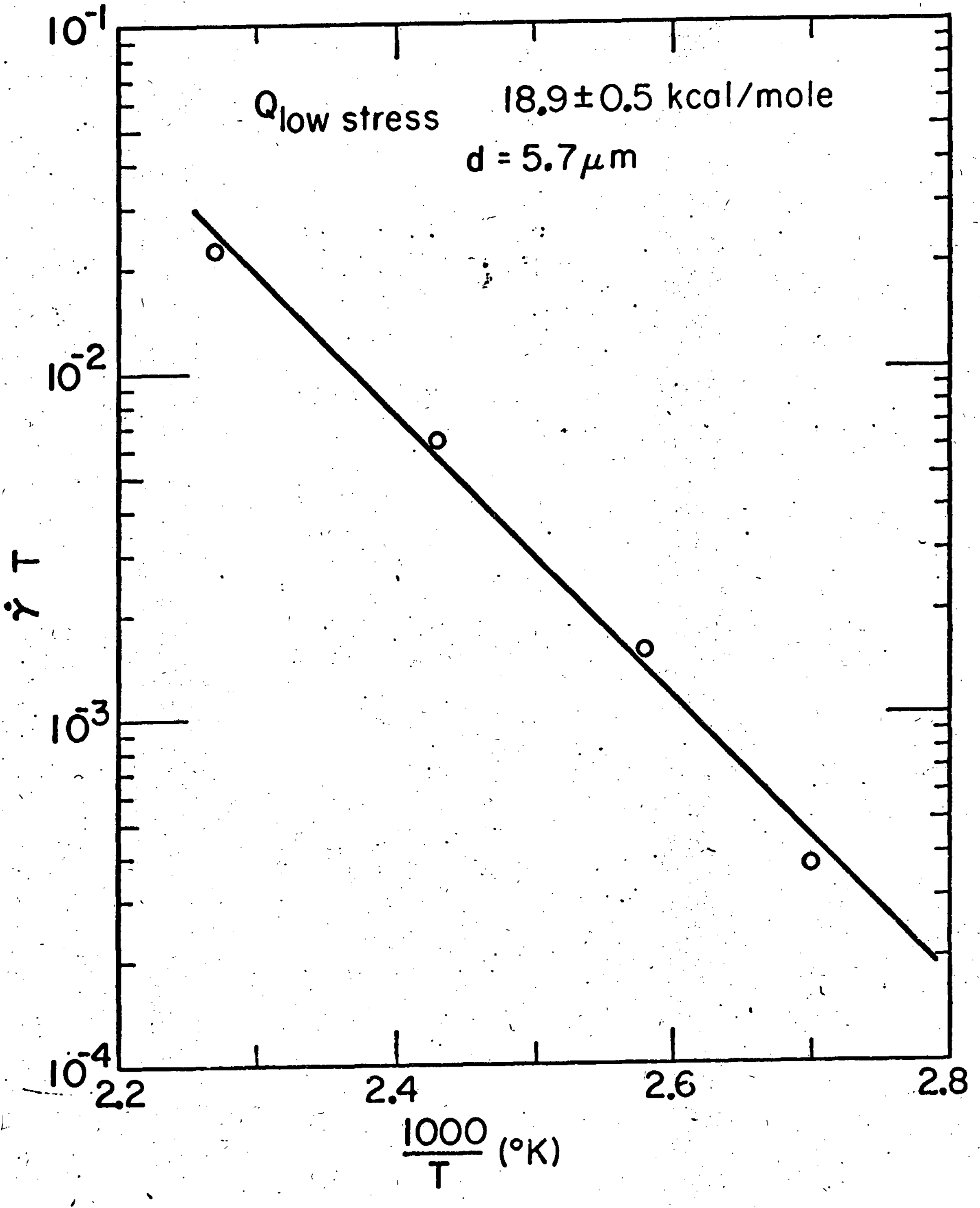

XBL7312-6969

Fig. 8. Arrhenius plot of ln$\dot{\gamma}$T vs 1000/T for the computation of the activation energy for the low stress creep region ($\dot{\gamma}$T is related to $\dot{\gamma}^*$ by a constant).

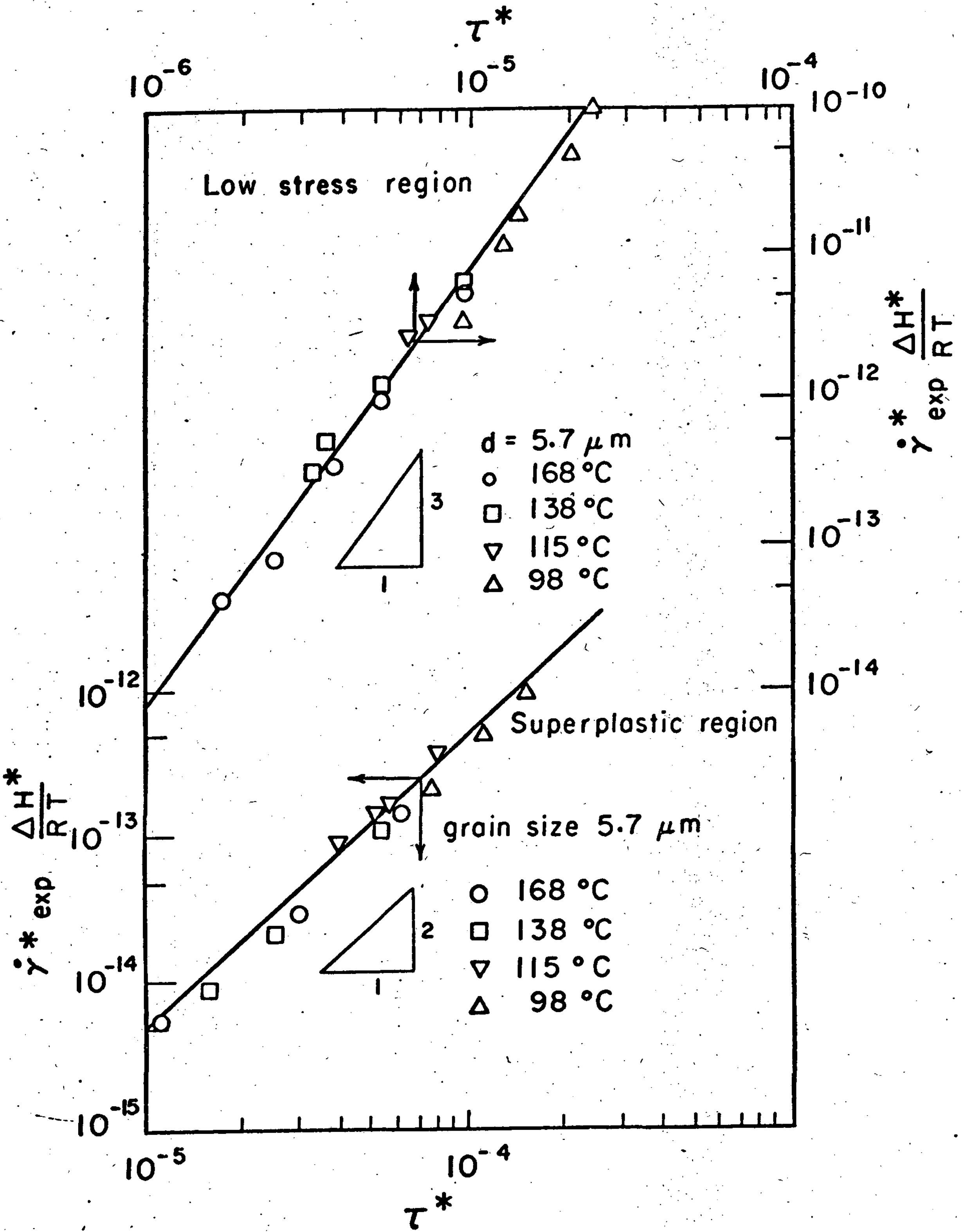

XBL7312-6987

Fig. 14. Temperature compensated plots of ln$\dot{\gamma}^*$ exp ($\Delta H^*/RT$) against ln τ^* for the 5.7 μm specimen in the superplastic and low stress regions.

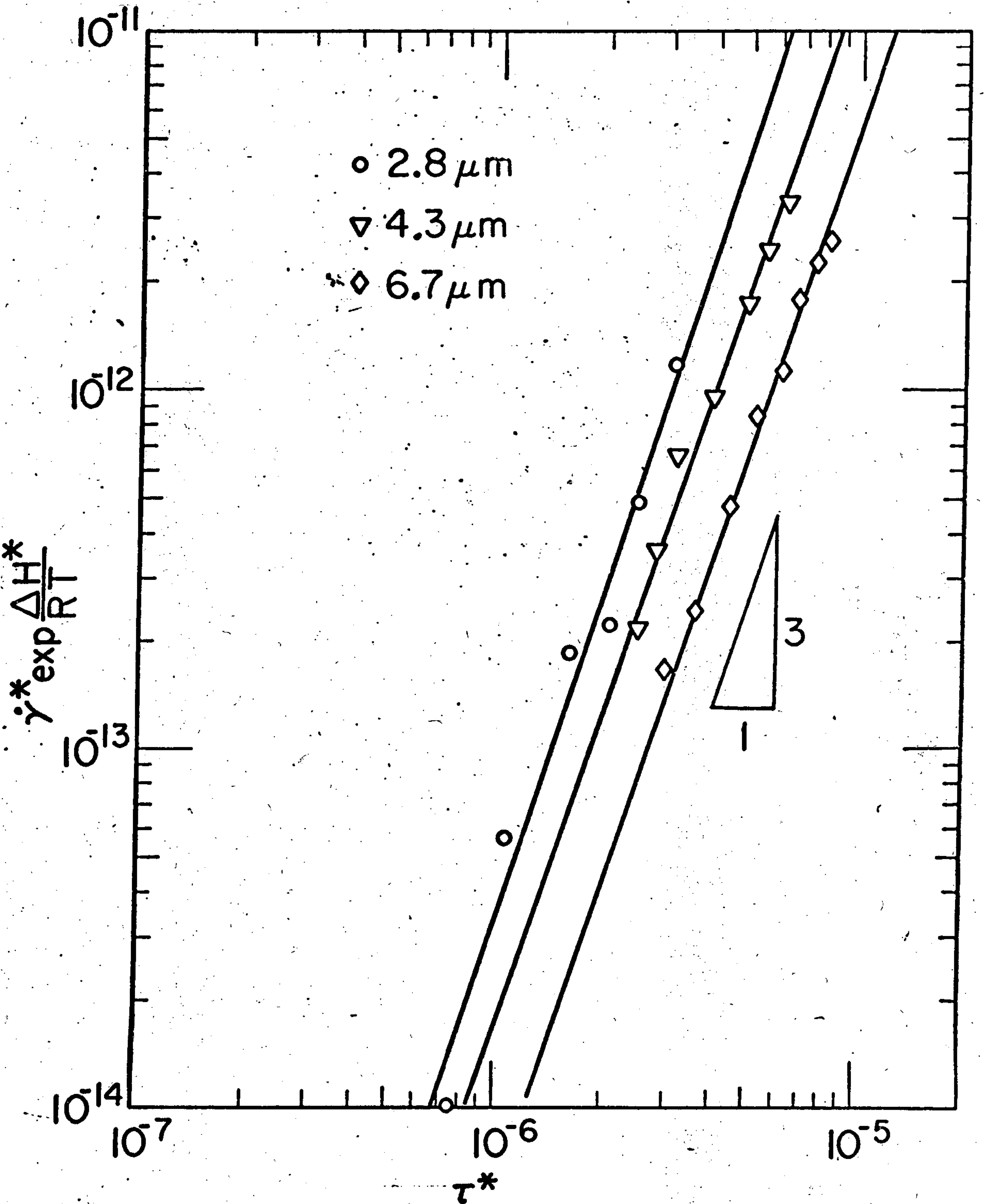

XBL 7312-6968

Fig. 5. A logarithmic plot of the temperature compensated strain rate against $\ln\tau^*$ for the 2.8 μm, 4.3 μm and 6.7 μm grain sizes.

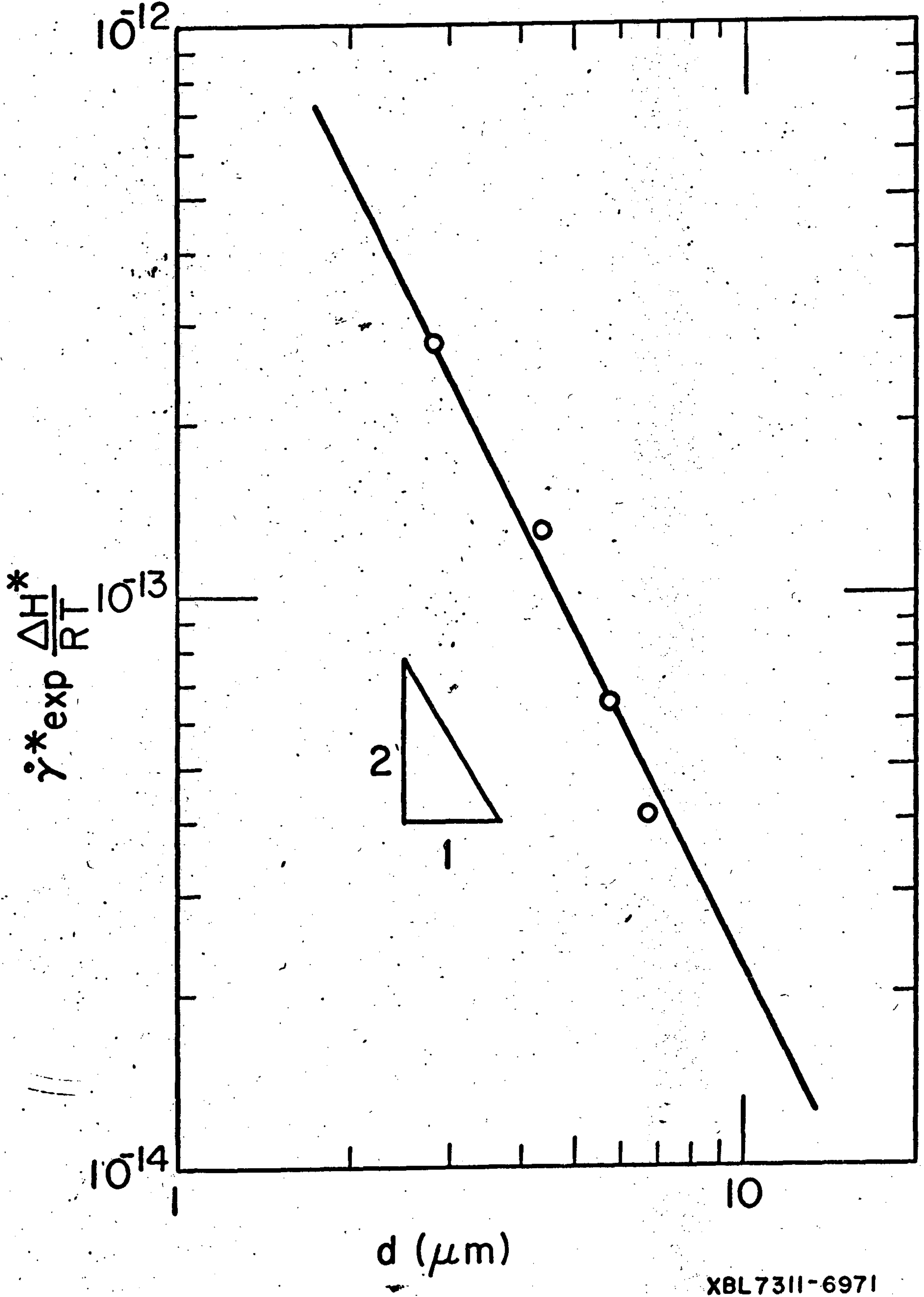

XBL7311-6971

Fig. 6. A plot of ln$\dot{\gamma}^*$ exp ($\Delta H^*/RT$) vs. lnd to determine the grain size dependence in the low stress creep region.

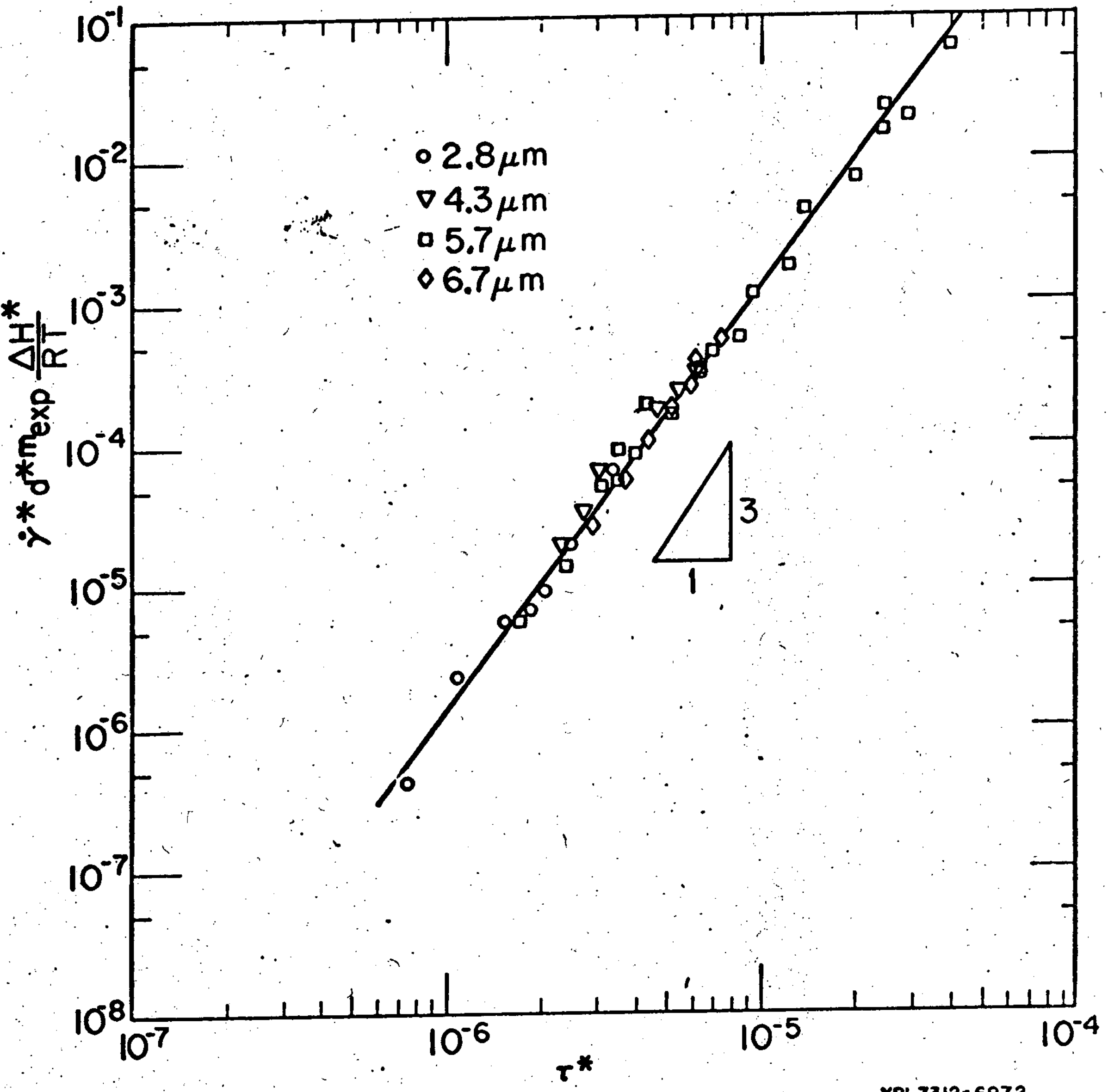

XBL7312-6972

Fig. 7. A logarithmic plot of the strain rate compensated for temperature and grain size against τ^*.

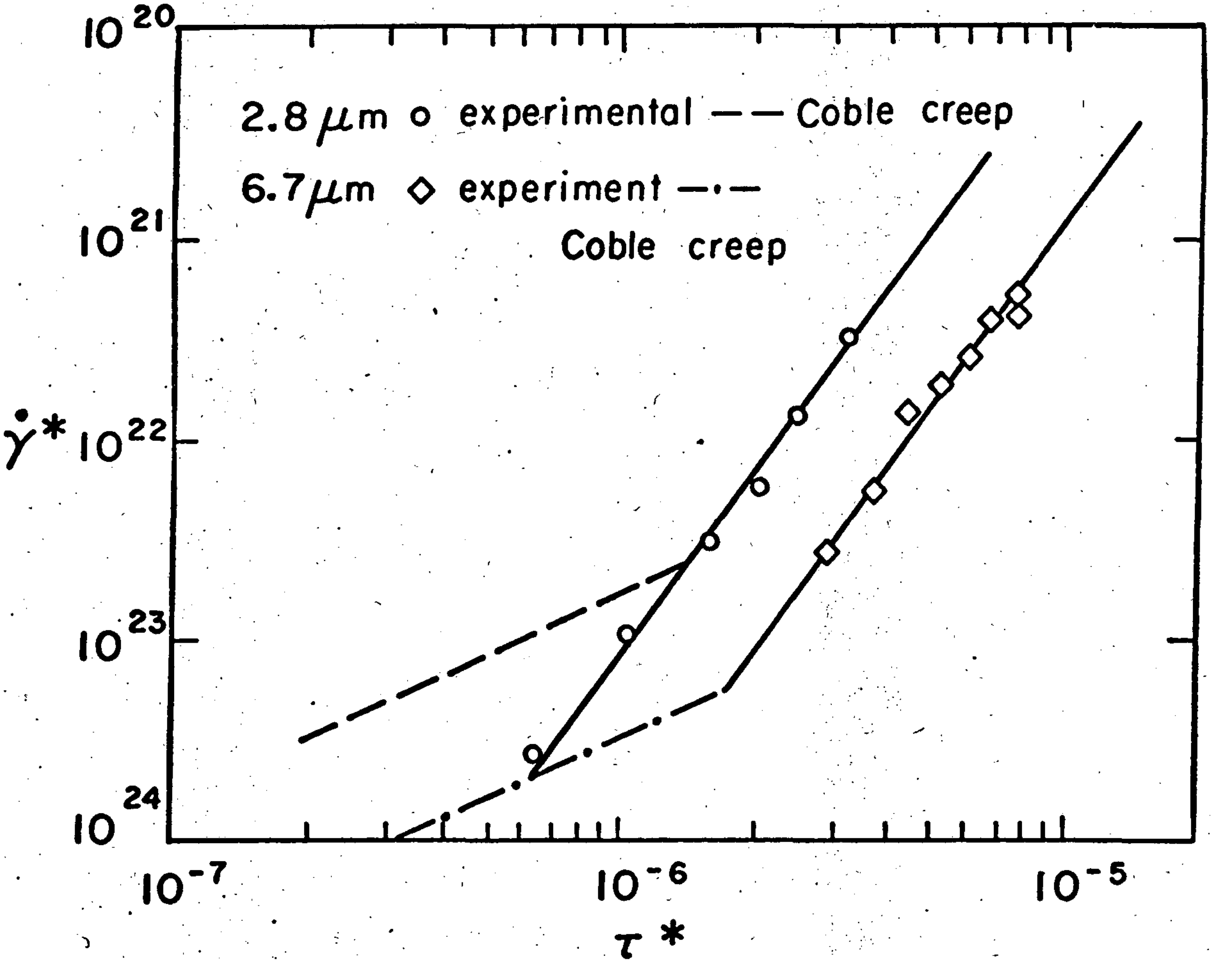

XBL 7312-7029

Fig. 8. The low stress region data for the 2.8 μm and 6.7 μm grain size including the Coble creep as introduced by Bird et al[1], $\dot{\gamma}^* = 48\ (\tau^*)\ (d^*)^{-3} e^{-11500/RT}$.

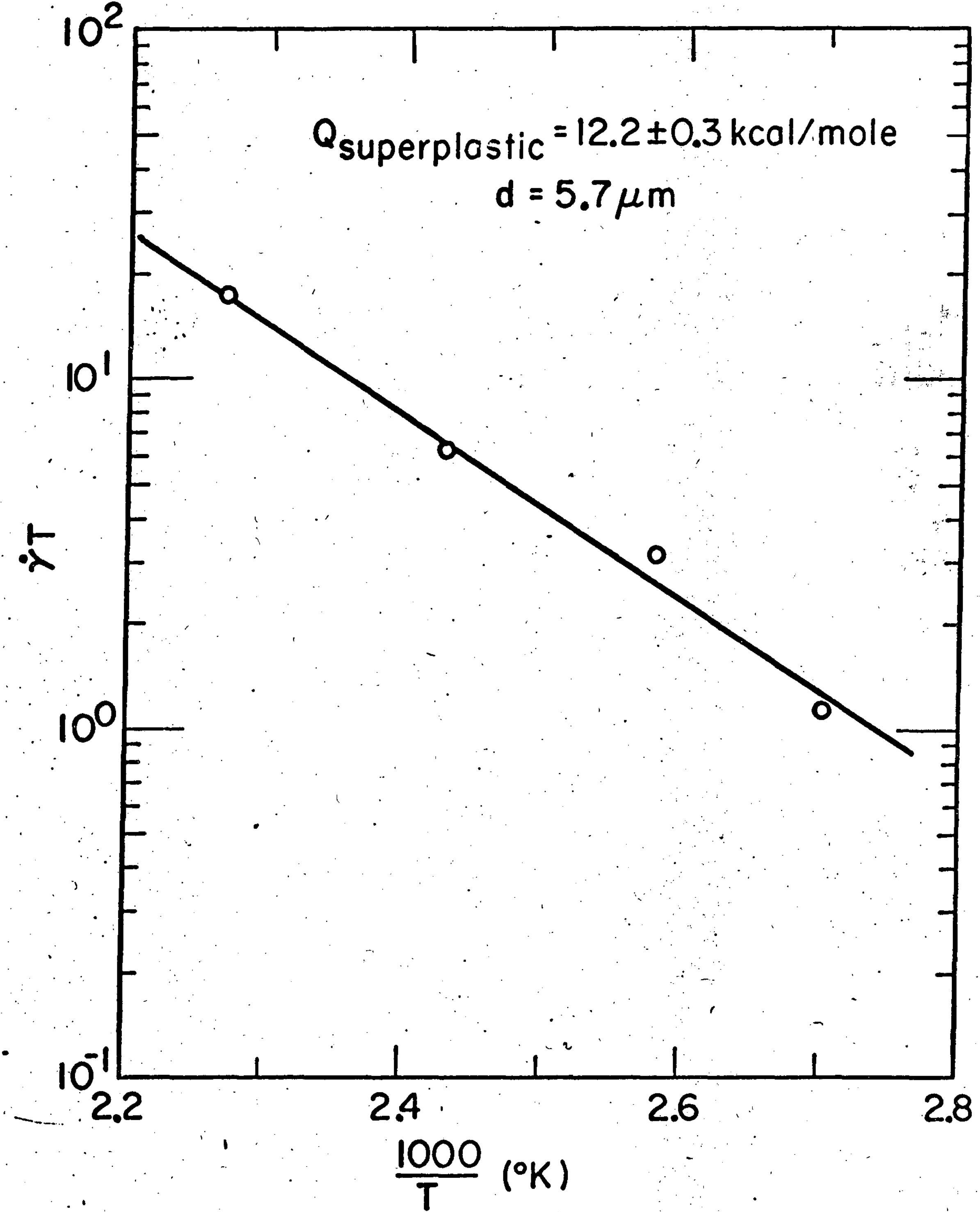

XBL7312-6970

Fig. 9. Arrhenius plot of $\ln\dot{\gamma}T$ against $^{1000}/T$ from which we compute the activation energy for the superplastic region.

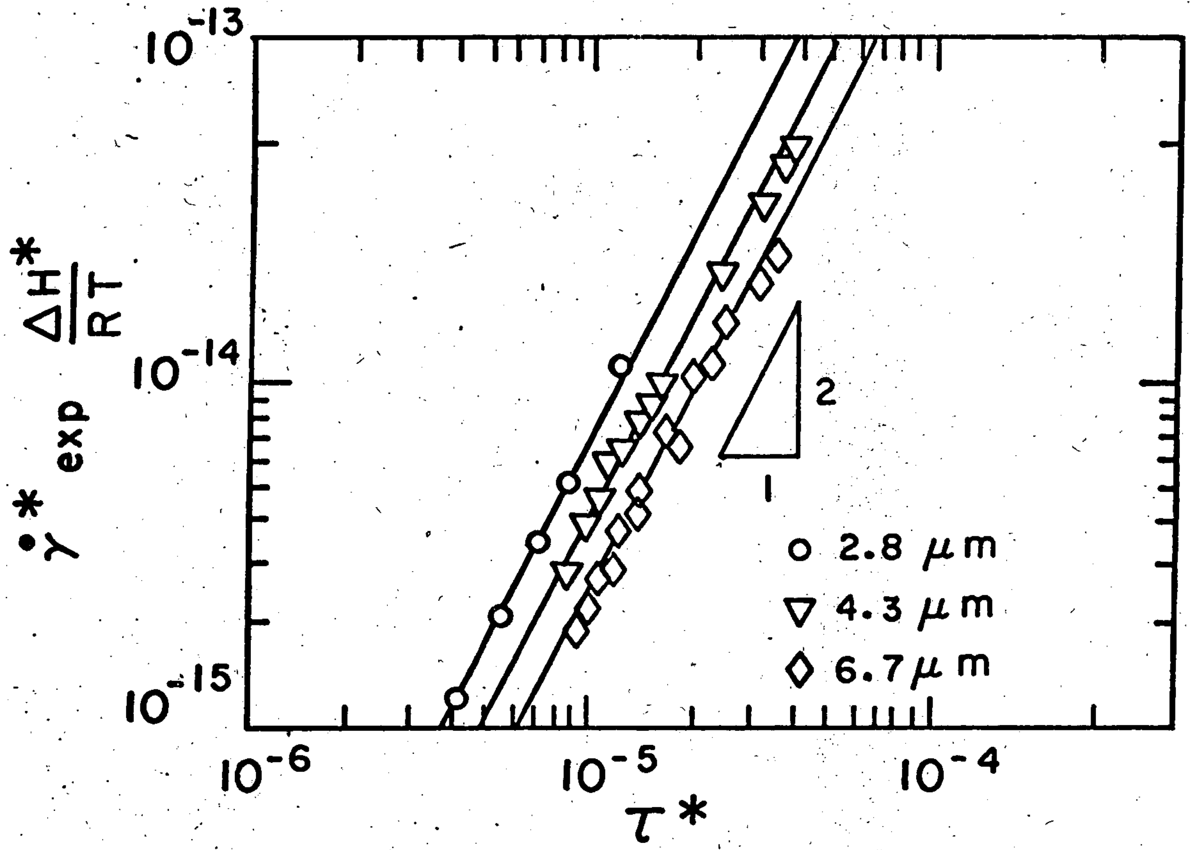

XBL7312-6988

Fig. 10. The logarithmic plot of the temperature compensated strain rate $\dot{\gamma}^*$ exp ($\Delta H^*/RT$) against τ^* for the 2.8 μm, 4.3 μm and 6.7 μm grain size.

TECHNICAL INFORMATION DIVISION
LAWRENCE BERKELEY LABORATORY
UNIVERSITY OF CALIFORNIA
BERKELEY, CALIFORNIA 94720